Activation of Two Sequential H Transfers in the Thymidylate Synthase Catalyzed Reaction

ARTICLE *in* ACS CATALYSIS · SEPTEMBER 2015

Impact Factor: 9.31 · DOI: 10.1021/acscatal.5b01332

ACS Catalysis

Research Article

pubs.acs.org/acscatalysis

Activation of Two Sequential H Transfers in the Thymidylate Synthase Catalyzed Reaction

Zahidul Islam,[†] Timothy S. Strutzenberg,[†] Ananda K. Ghosh,[†] and Amnon Kohen*[,†]

[†]The Department of Chemistry, The University of Iowa, Iowa City, Iowa 52242, United States

Supporting Information

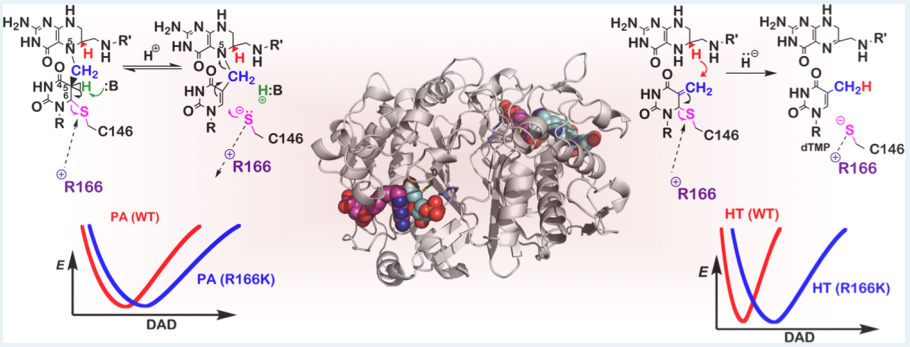

ABSTRACT: Thymidylate synthase (TSase) catalyzes the de novo biosynthesis of thymidylate, a precursor for DNA, and is thus an important target for chemotherapeutics and antibiotics. Two sequential C−H bond cleavages catalyzed by TSase are of particular interest: a reversible proton abstraction from the 2′-deoxyuridylate substrate, followed by an irreversible hydride transfer forming the thymidylate product. QM/MM calculations of the former predicted a mechanism in which the abstraction of the proton leads to formation of a novel nucleotide-folate intermediate that is not covalently bound to the enzyme (Wang, Z.; Ferrer, S.; Moliner, V.; Kohen, A. *Biochemistry* **2013**, 52, 2348−2358). Existence of such an intermediate would hold promise as a target for a new class of drugs. Calculations of the subsequent hydride transfer predicted a concerted H transfer and elimination of the enzymatic cysteine (Kanaan, N.; Ferrer, S.; Marti, S.; Garcia-Viloca, M.; Kohen, A.; Moliner, V. *J. Am. Chem. Soc.* **2011**, 133, 6692−6702). A key to both C−H activations is a highly conserved arginine (R166) that stabilizes the transition state of both H transfers. Here, we test these predictions by studying the R166-to-lysine mutant of *Escherichia coli* TSase (R166 K) using intrinsic kinetic isotope effects and their temperature dependence to assess effects of the mutation on both chemical steps. The findings confirmed the predictions made by the QM/MM calculations, implicate R166 as an integral component of both reaction coordinates, and thus provide critical support to the nucleotide-folate intermediate as a new target for rational drug design.

KEYWORDS: *thymidylate synthase, QM/MM calculations, kinetic isotope effect, C−H bond activation, phenomenological models, donor and acceptor distances, tunneling ready state*

Enzymes enhance the rate of reactions to an astounding extent, and a significant portion of the rate enhancements involve catalyzing formations and breakdowns of many otherwise stable chemical bonds, including the covalent bond between a carbon and a hydrogen (C−H bond). The molecular and physical details underlying enzyme-catalyzed C−H bond activations remain elusive, especially in enzymes that do not contain catalytic metals. Two such C−H bond activations are at the heart of the reaction catalyzed by thymidylate synthase (TSase), which is the de novo source of thymidylate (2′-deoxythymidine-5′-monophosphate, dTMP), one of the four DNA building blocks, in most organisms. TSase is a highly conserved enzyme, and 75% of 109 TSase sequences from pathogenic organisms were found to exhibit an overall identity of 40−80% with human TSase.[1] Cancerous cells overexpress TSase, and inhibition of TSase causes thymineless cell death, which has attracted the development of many chemotherapeutic drugs targeting this protein.[1−3] Derivatives of both pyrimidine (e.g., 5-fluorouracil) and folate (e.g., raltitexed) have long been used as chemotherapeutic drugs.[1,4] These drugs, however, exhibit toxicity, and their competency is limited because of the development of resistance.[2,5,6] The need for a new class of drugs that would target TSase in malignant cells stimulates a detailed investigation of structures and mechanism and the correlation between them.[1,3−5,7−10]

TSase catalyzes a net transfer of a methyl group from its cofactor 5,10-methylene-5,6,7,8-tetrahydrofolate (CH_2H_4folate) to the substrate 2′-deoxyuridine-5′-monophosphate (dUMP) to form dTMP and 5,6-dihydrofolate (H_2folate).[11] In its traditionally proposed mechanism (Scheme 1),[12,13] an active-site nucleophile cysteine (C146 in the

Received: June 25, 2015
Revised: August 30, 2015

DOI: 10.1021/acscatal.5b01332
ACS Catal. 2015, 5, 6061−6068

Scheme 1. Principle Mechanism of TSase

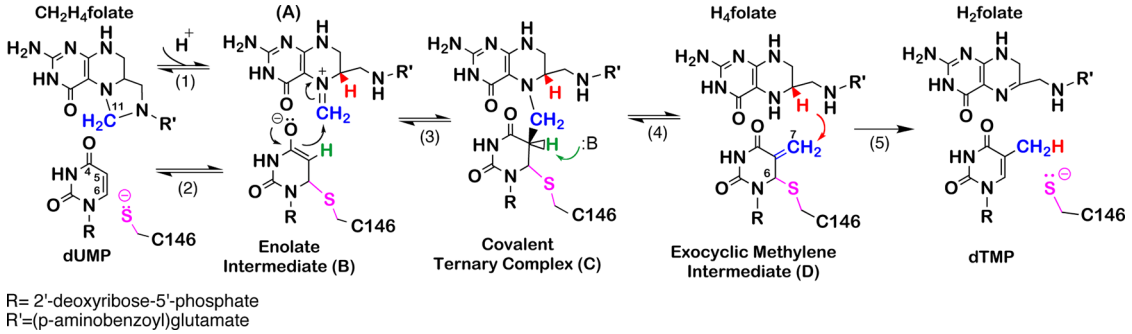

Scheme 2. Traditional (A) and Calculated[17,18] (B) Mechanisms for the Proton Abstraction and the Hydride Transfer in TSase[a]

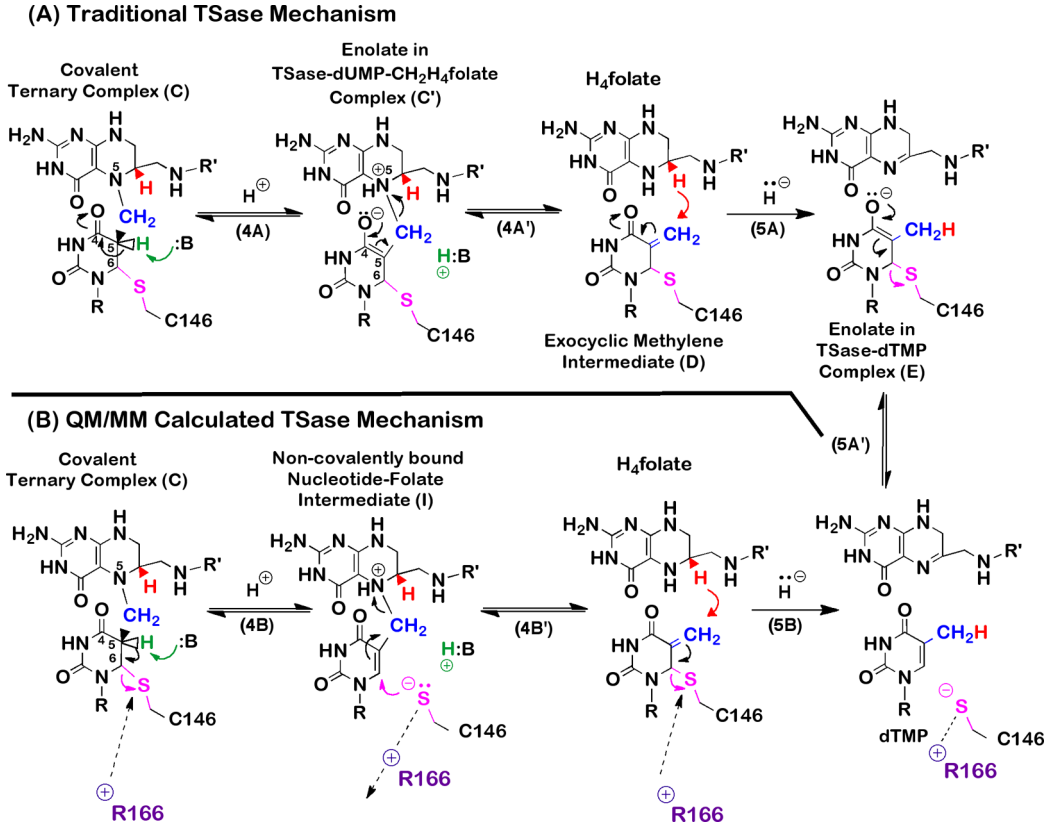

[a]In the QM/MM calculations, the abstraction of $C5_U$ proton induces the cleavage of S_{C146}–$C6_U$, leading to the formation of the nucleotide-folate intermediate. Following the protonation of the N5 of folate, the departed C146 then reattacks the nucleotide-folate intermediate, assisting in the succeeding β-elimination of the cofactor, generating the exocyclic methylene intermediate. Then the concerted hydride transfer and elimination of C146 leads to the product dTMP.

Escherichia coli TSase) initiates the reaction through Michael addition to C6 of dUMP ($C6_U$), forming an enzyme-bound substrate enolate intermediate (compound B in Scheme 1), which then attacks the preactivated CH_2H_4folate and forms a covalent ternary complex TSase–dUMP–CH_2H_4folate (compound C in Scheme 1). From this point, two chemical transformations lead to the formation of the final product dTMP: (i) a proton abstraction from the C5 of the pyrimidine base ($C5_U$), and the elimination of H_4folate from the bridging methylene, forming an exocyclic methylene intermediate (compound D in Scheme 1); and (ii) a hydride transfer from the C6 of H_4folate ($C6_F$) to the C7 of the methylene intermediate ($C7_E$) and the dissociation of the active site cysteine from the nucleotide, leading to the product dTMP. The hydride transfer is irreversible,[14,15] but the proton abstraction is fast and reversible. This difference in kinetic behavior of the two H transfers may suggest different physical natures of bond activations within the same enzymatic active site.[16]

Quantum mechanics/molecular mechanics (QM/MM) calculations have recently suggested that the traditional mechanism illustrated in Scheme 1 is missing some key features.[17−21] Calculations on the proton abstraction (step 4)[17,21] suggested that the covalent bond between the enzymatic nucleophile C146 and the pyrimidine dUMP (S_{C146}–$C6_U$) cleaves with the abstraction of the proton from the C5 of the dUMP, resulting in a Cys–thiol anion elimination from the C6 of the pyrimidine base, leading to the formation of a new and

DOI: 10.1021/acscatal.5b01332
ACS Catal. 2015, 5, 6061−6068

unexpected reaction intermediate that comprises the nucleotide and the folate and is not covalently bound to the enzyme (Scheme 2, compound I). Existing chemotherapeutic drugs targeting TSase are either derivatives of the pyrimidine (e.g., 5F-dUMP) or the folate (e.g., Raltiterxed); the proposed new nucleotide-folate intermediate presents a potential target for a new class of antibiotics and chemotherapeutics. Calculations[18,19] on the subsequent hydride transfer (step 5) predicted a concerted hydride transfer and C146 elimination to form the final product dTMP, whereas the traditional mechanism proposes a stepwise mechanism with the enolate as an intermediate (Scheme 2, compound E).[22] Key to both calculations was a highly conserved residue arginine (R166) that seems to stabilize the transition states for both the proton abstraction and the hydride transfer. The outcome of the QM/MM calculations indicates that R166 alternately fluctuates toward and away from the nucleophile thiol on C146 to stabilize it as a leaving group for each H transfer and to prepare it for the following nucleophilic attack, respectively (Scheme 2). In contrast to the traditional TSase mechanism,[11,13,22,23] these calculations predicted that the covalent bond between the substrate and the enzyme is quite labile as a result of the fluctuations of R166. The calculations also predicted that the coordinated motion between R166 and C146 and the resulting charge stabilizations at different transition states make R166 an inextricable part of the reaction coordinate for the both H transfers catalyzed by this enzyme.

Temperature dependence of intrinsic kinetic isotope effects (KIEs) has emerged as a powerful tool to probe the nature of C−H bond activations within complex cascades of chemical events.[24,25] This tool has been utilized to investigate C−H bond activations in the wild-type (WT) TSase.[15,16] It was found that the intrinsic KIEs on the hydride transfer (step 5 in Scheme 1) are temperature-independent, whereas those on the proton abstraction (step 4) are steeply temperature-dependent.[15,16] Phenomenological models offer an interpretation of these kinetic results.[24−33] In these models, because the transferring particle (hydrogen) is rather light, quantum mechanical tunneling occurs between the H donor and the H acceptor when the wave functions for the hydrogen atom in the reactant and product wells overlap with each other. The space along the reaction coordinates where the energy of the donor and acceptor well are degenerate and tunneling probability is more than zero is called "Tunneling Ready State" (TRS), which is merely the quantum mechanically delocalized transition state (TS).[24,34,35] Motions of the protein, reactants, and solvent bring the system to the TRS and modulate tunneling by altering the height and width of the energy barrier between the reactant and the product states. The expression of KIE in the framework of these activated tunneling models is given by eq 1 and is illustrated in Figure 1:[24,36]

$$KIE = \frac{\int_0^{\infty} P_{DAD}^{l} e^{-(E_{DAD}/k_b T)}\, dDAD}{\int_0^{\infty} P_{DAD}^{h} e^{-(E_{DAD}/k_b T)}\, dDAD} \quad (1)$$

where P_{DAD}^{l} and P_{DAD}^{h} are the transfer probabilities for the light and heavy atoms, which depend on their respective masses; and the exponential term is the Boltzmann factor representing a distribution of H donor and acceptor distances (DADs) at the TRS. From eq 1, the DADs and their distributions at TRS determine both the magnitude and the temperature dependence of KIEs. In the framework of this model, temperature-independent KIEs stem from a narrow distribution of DADs at the TRS (well reorganized TS), and the temperature-dependent KIEs result from a broader distribution of DADs at the TRS (poorly reorganized dividing line between donor and acceptor with broad ensemble of TSs). In *E. coli* TSase, the hydride transfer (step 5 in Scheme 1) has a narrow distribution of DADs, as reflected by temperature-independent KIEs, whereas the fast proton abstraction (step 4) has a broader distribution of DADs, as reflected by temperature-dependent intrinsic KIEs.[16] Mutation of residue(s) that is(are) part of the reaction coordinate of a certain H transfer changes the geometry of the TRS and, thereby, the distribution of DADs, which is commonly manifested as a change in the temperature dependence of KIEs for that mutant.[24,37] Thus, a mutation that results in a change in the temperature dependence of intrinsic KIEs serves as an indication that the residue in the wild-type (WT) enzyme was likely part of the reaction coordinate under study.

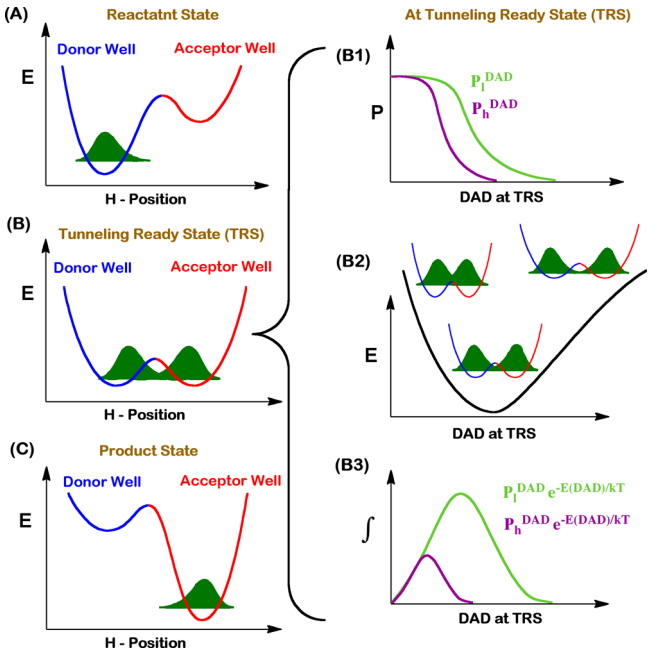

Figure 1. Phenomenological models for activated H tunneling. Left column represents three stages of the reaction along the H transfer coordinate. Motion of the protein, solvent, and reactants modulate the potential energy surfaces for the H transfer. At the reactant state (A), the H wave function is localized in the donor well. The motion of the heavy atoms transiently brings the donor and the acceptor wells into the tunneling ready state (TRS, B), where isotopically sensitive H transfer from donor to acceptor occurs. Further rearrangement in the heavy atoms interrupts the TRS, resulting in entrapment of the hydrogen in the product well (C). The right column demonstrates the contributing factors that modulate H transfer probability at the TRS. The panel B1 shows the transmission probabilities of light (l, green) and heavy (h, purple) hydrogen isotopes as a function of DAD. Panel B2 represents a potential energy surface (PES) for the DAD fluctuations. Panel B3 shows the product of DADs and transmission probabilities.

Although the role of R166 in activating C146 to initiate the catalytic cycle by Michael addition of C146 to the nucleotide was proposed in the traditional mechanism,[11,13] the catalytic role of R166 in the subsequent H transfers was delineated only in the calculated mechanisms.[17,18,21] Here, we report experimental examination of these QM/MM predictions, by

DOI: 10.1021/acscatal.5b01332
ACS Catal. 2015, 5, 6061−6068

comparing intrinsic KIEs and their temperature dependence for the proton and the hydride transfers for the WT and R166 K mutant of *E. coli* TSase. The experimental findings confirm and characterize the role of R166 in both C−H bond activations and consequently provide a critical experimental support for the calculated mechanisms. The findings thus reinforce the existence of an unexpected noncovalently bound intermediate that combines the folate and nucleotide moieties.

MATERIALS AND METHODS

Chemicals. All chemicals, including deoxyuridine monophosphate (dUMP), 5-fluorodeoxyuridine monophosphate (5-FdUMP), and tris(2-carboxyethyl)phosphine (TCEP), were purchased from Sigma-Aldrich, St. Louis, MO, unless otherwise mentioned. [6-^{3}H]dUMP and [2-^{14}C]dUMP were purchased from Moravek Biochemicals. Unlabeled 5,10-methylene-5,6,7,8-tetrahydrofolate (CH_2H_4folate) was generously donated by EPROVA (Switzerland). [^{3}H]$NaBH_4$ and [^{2}H]$NaBH_4$ were purchased from American Radiolabeled Chemicals and Cambridge Isotopes, respectively. [2-^{x}H]*i*PrOH was synthesized by reduction of acetone with [^{x}H]$NaBH_4$. Dihydrofolate was prepared according to the Blakley method.[38] Ultima Gold liquid scintillation cocktail and scintillation vials were purchased from Packard Biosciences and Research Products International, respectively. Wild-type (WT) and mutant R166 K *E. coli* TSase were expressed and purified according to a previously described procedure.[39] Steady-state initial velocities were determined using a Hewlett-Packard model 8452A diode-array spectrophotometer equipped with a temperature-controlled cuvette assembly. All separations were accomplished using an Agilent Technologies 1100 HPLC system with Supelco Discovery C18 reversed phase analytical or semipreparative columns. Radioactive samples were analyzed using a liquid scintillation counter (LSC).

Synthesis of [2-^{14}C,5-^{2}H]dUMP and for Proton Transfer KIE Experiments. [2-^{14}C,5-^{2}H] dUMP was prepared using a methodology developed by Wataya and Hayatsu.[40] Briefly, 1 mM [2-^{14}C]dUMP is incubated with 1 M L-cysteine in (>99.96% D) D_2O, pD 8.8, at 37 °C. Deuteration of $C5_U$ was followed by ^{1}H NMR and verified as completed after 7 days of incubation. Aliquots of the reaction mixture were then stored at −80 °C until used in later proton abstraction D/T KIE experiments. Interestingly, one should note that TSase also activates the $C6_U$ position of dUMP by nucleophilic attack of active site residue C146 on $C5_U$ of dUMP.

Competitive Primary KIE Experiments. The competitive primary (1°) KIE experiments for the proton transfer step in R166 K followed the same conditions as used previously to measure the proton transfer KIEs for the WT enzyme.[16] Briefly, the reaction mixture contained 2 mM TCEP, 1 mM EDTA, 5 mM HCHO, and 50 mM $MgCl_2$ in addition to the substrates and the enzymes. CH_2H_4folate is taken in ∼25−30% excess to dUMP (1.35 mM) and the mixture buffered in 100 mM Tris. In addition, trace amounts of [5-^{3}H]dUMP, with [2-^{14}C]dUMP or [2-^{14}C,5-^{2}H]dUMP for H/T and D/T KIE experiments, respectively, are added such that the ratio of ^{3}H to ^{14}C in the reaction mixture was kept above 6.0 for higher accuracies in the LSC analyses. Aliquots of the reaction mixture were equilibrated to 5, 15, 25, or 35 °C, the pH was adjusted to 7.5 at the respective temperature, and the reaction was initiated with ∼100−300 μM R166 K TSase. Throughout the course of the reactions, six aliquots were removed at different time points (t), when fraction conversion was between 25 and 80%. These aliquots were immediately quenched with excess 5-FdUMP, a tight-binding competitive inhibitor of TSase, and stored at −80 °C until later analysis. In addition to these reaction mixtures, three aliquots at 0% conversion (t_0) controls and three aliquots at 100% conversion (t_{inf}), were collected by incubating the reaction mixture overnight with WT TSase at 35 °C. Reactants and products of each aliquot were separated by RP HPLC, and their radioactivity was measured by LSC. From the ^{14}C radioactivity of the reactants and products, fraction conversions (f) can be determined according to eq 2. In addition, the ratio of ^{3}H to ^{14}C in the products of the time points (R_t) and time infinity (R_{inf}) was used to determine the observed KIE using eq 3, whose derivation is described elsewhere.[41]

$$f = \frac{[^{14}\text{C}]\text{dTMP}}{[^{14}\text{C}]\text{dUMP} + [^{14}\text{C}]\text{dTMP}} \tag{2}$$

$$\text{KIE}_{obs} = \frac{\ln(1-f)}{\ln\left[1 - f\left(\frac{R_t}{R_{inf}}\right)\right]} \tag{3}$$

Because, in contrast to the hydride transfer step, the proton abstraction is reversible, further analysis is needed to avoid artifacts. Although tritium and deuterium abstractions are practically irreversible (due to dilution into H_2O), the formed intermediate could be followed by reversible protonation of the C5-dUMP. When this reversible step effectively competes with the forward reaction, an up-going trend for the D/T KIE_{obs} is observed, ranging from the actual D/T KIE_{obs} value at early fraction conversion ($f \rightarrow 0$) to H/T KIE_{obs} at late fraction conversion ($f \rightarrow 1$). Although this phenomenon has been observed for other mutants (data not shown), a plot of KIE_{obs} as a function of f for both R166 K and the WT TSase (Figure S1) shows no such trend. This finding suggests that the forward H transfer rate and the subsequent irreversible formation of the product were dominant compared with the rate of reverse reaction. Furthermore, for KIEs on the proton abstraction, both the reversibility and the fact that CH_2H_4folate inflates the commitment[43] deflate the KIE_{obs}. However, the Northrop method used to calculate the intrinsic KIEs (eq 4 below) drops the commitment factor out of the final outcome, as discussed in the following section (Intrinsic KIEs).

The experimental details for the KIE_{obs} on the hydride transfer were reported in ref 42. In brief, [6R-^{x}H]CH_2H_4folate (^{x}H = D and T) was synthesized according to the procedure described in ref 15. The competitive H/T and D/T KIE_{obs} on the hydride transfer were measured using H/T- and D/T-labeled CH_2H_4folate, and the reaction was carried out under the same conditions as for the proton abstraction measurements described above.

Intrinsic KIEs. Intrinsic KIEs were calculated from their observed values using the Northrop method as described in refs 16 and 41. Briefly, in this method, a combination of KIEs (H/T and D/T in the current case) is measured, in which the hydrogen isotope common to both KIE measurements (T) serves as the reference isotope.[43] For the H/T and D/T KIE measurements, the Northrop method uses eq 4, which allows extracting the intrinsic KIEs by eliminating the commitment to catalysis on the reference isotope, T.[35,41]

DOI: 10.1021/acscatal.5b01332
ACS Catal. 2015, 5, 6061−6068

$$\frac{{}^{T}(V/K)^{-1}_{H,obs} - 1}{{}^{T}(V/K)^{-1}_{D,obs} - 1} = \frac{\left(\frac{k_H}{k_T}\right)^{-1} - 1}{\left(\frac{k_H}{k_T}\right)^{-1/3.34} - 1} \quad (4)$$

Here ${}^{T}(V/K)_{H,obs}$, ${}^{T}(V/K)_{D,obs}$, and (k_H/k_T) are the observed H/T, D/T, and intrinsic KIEs, respectively. To calculate the intrinsic KIEs, a program freely available at http://chem.uiowa.edu/kohen-research-group/calculation-intrinsic-isotope-effects numerically solved eq 4 and extracted the intrinsic KIEs (KIE_{int}) with every combination of the observed values at a particular temperature. The intrinsic KIEs were then exponentially fitted to a modified Arrhenius equation where weighted root means square exponential regression (KaleidaGraph version 4.03) yields the KIE on Arrhenius pre-exponential factor (A_L/A_H) as well as the isotope effect on activation energies (ΔE_a) for the respective isotope comparisons.

RESULTS AND DISCUSSION

Activation of Two Sequential C−H Bonds. Observed KIEs on the proton abstraction for the WT TSase depend on the concentration of the second binding ligand CH_2H_4folate and reaches unity at high CH_2H_4folate concentration, indicating an ordered-binding mechanism.[16,43,44] However, for the mutant R166 K, a high concentration of CH_2H_4folate yields an observed KIE larger than unity, suggesting the mutation caused a more random binding mechanism, which was also observed for other mutants.[45,43] This observation agrees with steady-state kinetics with R166 K that demonstrated inflated K_M's for both the substrate and cofactor.[42] This can be rationalized by examination of WT crystal structures, in which the residue R166 forms two hydrogen bonds with the phosphate of the dUMP. The mutation to lysine thereby is likely to destabilize those tie-ups, reducing the affinity for dUMP and causing an overall disruption of the original order of binding preferences. Steady-state kinetic measurements indicate that this mutation reduced the turnover rate (k_{cat}) by ~90-fold and increased K_M for dUMP and CH_2H_4folate by more than 300- and 18-fold, respectively.[42]

To investigate how R166 modulates the C−H bond activation, KIEs and their temperature dependence were measured on both the hydride transfer and the proton abstraction for its only active variant, R166 K. Competitive KIEs (H/T and D/T) that report on the second-order rate constant (k_{cat}/K_m)[41] were measured at temperatures ranging from 5 to 35 °C (Table S1). The intrinsic KIEs, which are often masked by kinetic complexity, were extracted from the observed KIEs using the Northrop method.[35,41,46,47] Figure 2 shows an Arrhenius plot of intrinsic KIEs on the proton abstraction (red) and the hydride transfer (blue) for both the WT and R166 K TSase. Isotope effects on the activation energy ($\Delta E_{a,T/H}$) and on the pre-exponential factor (A_H/A_T) were obtained from the fittings of KIE data into the following Arrhenius equation:

$$KIE_{int} = \frac{k_H}{k_T} = \frac{A_H}{A_T}\exp\left(-\frac{\Delta E_{a,T/H}}{RT}\right) \quad (5)$$

where H and T denotes hydrogen and tritium, respectively.

As evident from Figure 2 and Table 1, the mutation of R166 increases the temperature dependence of KIEs for both the hydride transfer and the proton abstraction. In R166 K, the intrinsic KIEs on the hydride transfer become temperature-dependent while, for the proton abstraction, the temperature dependency becomes steeper (higher $\Delta E_{a,T/H}$) compared with that for the WT. The mutation also caused a significant increase in the magnitude of intrinsic KIEs for both H transfers across the examined temperatures. This observation is consistent with R166 in the WT TSase being a component of the reaction coordinate and the TS for both hydride and proton transfers, as predicted by the QM/MM calculations discussed above.

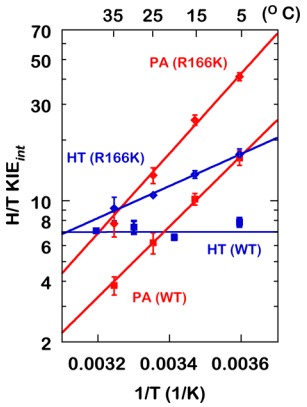

Figure 2. Arrhenius plots of intrinsic H/T KIEs on the proton abstraction (PA, red) and the hydride transfer (HT, blue)[15,42] for the WT (squares)[16] and R166 K (diamonds) TSase.

Table 1. Isotope Effects on the Activation Energy ($\Delta E_{a,T/H}$) and the Arrhenius Preexponential Factor (A_H/A_T) for the Proton Abstraction (PA) and the Hydride Transfer (HT) in the WT and R166 K

	$\Delta E_{a,T/H}$ (kcal/mol)	A_H/A_T
PA (WT)[16]	8.0 (±0.16)	8.3 (±1.0) × 10^{-6}
PA (R166 K)	9.0 (±0.10)	3.30 (±1.4) × 10^{-6}
HT (WT)[15]	0.02 (±0.25)	6.8 (±2.80)
HT (R166 K)[42]	3.62 (±0.02)	0.023 (±0.003)

In the framework of phenomenological models discussed above,[24,25,34,37] the larger magnitudes and the greater temperature dependences of KIEs indicate a larger average DAD and a broader DAD distribution, respectively. Figure 3 shows schematic illustrations of DAD distributions in terms of potential energy surfaces (PES) along the DAD coordinate at the TRS for the hydride transfer (left) and the proton abstraction (right) in both the WT and R166 K TSases. A stiff PES (large force constant and high DAD sampling frequency) represents a narrowly distributed ensemble of DADs, suggesting a well-defined TRS, as in the case for the hydride transfer for the WT TSase. A wide PES, on the other hand, corresponds to a less-organized TRS (small force constant and

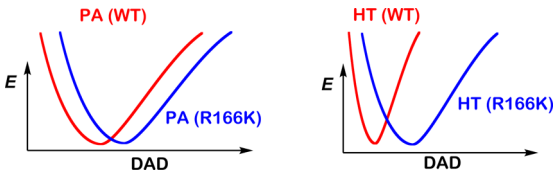

Figure 3. Illustration of potential energy surfaces (PESs) along the donor−acceptor distance (DAD) coordinate in TRS for WT (red) and R166 K (blue) TSase catalyzed proton abstraction (PA) and hydride transfer (HT) reactions. The relative changes in the distribution of DADs are demonstrated.

DOI: 10.1021/acscatal.5b01332
ACS Catal. 2015, 5, 6061−6068

low DAD sampling frequency), as in the case for the proton abstraction. These DADs' PESs are wider in the mutant R166 K (larger $\Delta E_{a,T/H}$), demonstrating perturbations to the TRSs caused by the mutation. The minima of these PESs representing the average DADs at the TRS shift toward larger DADs in the mutant R166 K. These combined features, the larger average DAD and the broad distribution of DADs, would explain both the inflated magnitude and the temperature dependence of the intrinsic KIEs in the mutant. An interpretation consistent with the QM/MM calculations would be that the mutation caused a disruption in the coordinated motion between R166 and C146 and in the following charge stabilizations, affecting both the hydride transfer and the proton abstraction reaction coordinate. It is important to note that alternative explanations, such as a coincidental similar remote effect of R166 on the TS of both C−H activations, cannot be excluded on the basis of the experimental observations alone; however, Ockham's razor should prefer one mechanism that explains both similar effects, as offered by the R166 role in activating C146 for both steps, which also agrees with the calculations. It is also important to note that several mutations closer to the reactions' center had no or a much smaller effect on the intrinsic KIEs or their temperature dependence relative to R166 K (e.g., W80M or Y209F)[43,45,48,49] In contrast to R166, residues W80 and Y209 were not predicted by the QM/MM calculations to be part of the reaction coordinate for either H transfers; thus, their lack of effect on these transfers may serve as an important control, further supporting the validity of the mechanism proposed in Scheme 2B.

To graphically present the effect of R166 K on both C−H activations, the isotope effects on the activation parameters from Table 1 are illustrated in Figure 4, which shows a plot of

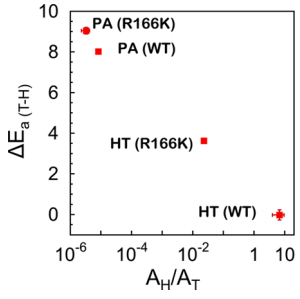

Figure 4. Presentation of the interrelation between isotope effects on activation parameters in the two H transfers catalyzed by the WT and R166 K TSases.

the isotope effects on the activation enthalpy ($\Delta E_{a,T/H}$) against the isotope effects on Arrhenius pre-exponential factors (A_H/A_T). Within TS theory, these two parameters are independent of each other, and no theoretical model predicts a trend between them. From Figure 4, it appears that the isotope effects on $\Delta E_{a,T/H}$ and A_H/A_T for both H transfers are oppositely affected by the mutation, indicating similar perturbations of their respective reaction coordinates in this case. In addition, it seems that the effect of the mutation on the hydride transfer is greater than for the proton abstraction, as evident from the higher magnitude of $\Delta E_{a,T/H}$ in R166 K for the former. This can be rationalized by the hydride transfer being slower in the WT,[14,15] thus requiring more assistance by R166 for the activation of the $S_{C146}-C6_U$ bond than that for the faster proton abstraction. That rationale is similar to the one that explains why the proton abstraction has a broad DAD distribution in the WT, that is, proton abstraction can happen without the enzyme catalysis, and thus, the enzyme need not force accurate TS and narrow DAD distribution. In stark contrast, the slower hydride transfer requires the enzyme to provide strict control over the TS, creating a narrow DAD distribution for that step.

Role of R166 in the Reversal of C146 Nucleotide Covalent Adduct. C146 is the active-site nucleophile that initiates the catalysis by Michael addition to C6 of dUMP. In the traditional mechanism of TSase, C146 remains covalently bonded to the substrate dUMP until the very last step of the reaction (steps 1−5, Scheme 1);[11,13] however, in the QM/MM calculated mechanisms, the $S_{C146}-C6_U$ bond was found to be very labile, and it alternates between a full and no covalent bond at different stages of the reaction.[17,18,21,50] Montfort et al.[51] also proposed an unstable nucleotide−C146 conjugate following an observation of a diffused electron density between the C6 in 5FdUMP and C146 in a crystal structure of TSase−5FdUMP−CH_2H_4folate complex (1TSN), even though a more stable $S_{C146}-C6_U$ bond (relative to the one with dUMP ligand) would be expected as a result of the strong electron-withdrawing potential of fluorine in the 5FdUMP. The diffused electron density around $S_{C146}-C6_U$ was also observed in several other ternary complexes (e.g., 3BHL, 1KZI, 2G8O), supporting a labile $S_{C146}-C6_U$ conjugate.

Another key feature in the traditional mechanism includes the formation of enolates in the binary (compound B in Scheme 1 and compound E in Scheme 2) and ternary complexes (compound C′ in Scheme 2).[11−13,22,23] In the crystal structure of TSase, the side chain of N177 is found to be situated within the hydrogen bonding distance to the C4═O4 of dUMP (Figure 5), presumably stabilizing the charge on the

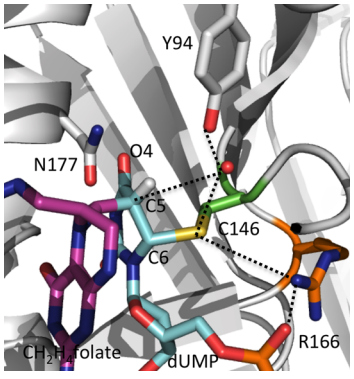

Figure 5. Active site structure of TSase covalently bound with 5-fluoro dUMP and CH_2H_4folate (PDB ID 1TLS). The ligands (dUMP, CH_2H_4folate) and residues close to the H transfers' site are shown in sticks, and atoms that were predicted to interact during the catalytic cycle are connected by dashed lines.

oxyanion. Nevertheless, in the calculations,[17,18] both H transfers were found to occur through mechanisms that bypass complete enolate formations and only suggested some negative charge accumulation at that carbonyl.[17,18] A recently reported normal secondary KIE (2°) on the C6 of dUMP for the conversion of the exocyclic methylene intermediate to dTMP in the WT TSase indeed supported a concerted hydride transfer.[42] Importantly, this experimental 2° KIE was recently reproduced by a QM/MM calculation.[50] Another recent high

DOI: 10.1021/acscatal.5b01332
ACS Catal. 2015, 5, 6061−6068

level QM/MM calculation carried out by an independent group[52] on the formation of the covalently bonded ternary complex from the noncovalent one (from step 1 to step 3 in Scheme 1) supported a previous report[21] suggesting that the initial Michael addition and the covalent ternary complex formation (compound C′ in Scheme 2) are also concerted. In this recent and independent calculation,[52] R166 was also found to promote the concerted process that bypasses the initial enolate in the binary TSase−dUMP complex (compound B in Scheme 1).

CONCLUSIONS

Understanding the role of protein motions in the chemical bond activation, particularly for C−H bonds, is of contemporary interest. TSase catalyzes a series of cleavages and formations of chemical bonds, including two C−H bond activations. The studies presented above tested predictions by the QM/MM calculations[17,18] that proposed alternative mechanisms for the two different C−H bond activations catalyzed by the same active site. By these calculations, residue R166 is central for both hydride and proton transfers. It was suggested that TSase exploits the reversals of C146−nucleotide adduct coordinated by R166 motions to catalyze the breaking of several covalent bonds. Indeed, R166 has been ranked as one of the five most essential residues for the catalysis because the enzyme cannot tolerate any substitution at this position other than lysine.[13] The intrinsic KIEs and their temperature dependence on the proton abstraction and the hydride transfer presented above implicate R166 as an important component of both H transfers' coordinates and thus support the QM/MM calculation-predicted role of R166 in these H transfers. It seems that R166 plays three possible roles in catalysis: (i) activating C146 to initiate the Michael addition (step 2 in Scheme 1), as proposed in the traditional mechanism,[13] which was also supported by the QM/MM calculations;[21,52] (ii) facilitating the proton abstraction by promoting the cleavage of S_{C146}−$C6_U$, forming a newly predicted nucleotide-folate intermediate; and (iii) assisting the concerted hydride transfer. The last two roles were first predicted by the QM/MM calculations and are now corroborated by the experiments presented above. The alternative mechanism for the proton abstraction has an important significance because it proposes a new nucleotide-folate intermediate that is not covalently bound to the enzyme. Such an intermediate, if it exists, could represent a new target for designing TSase inhibitors as leads toward a new class of antibiotics and chemotherapeutics. The current kinetic data support the steps before (the proton abstraction, 4B in Scheme 2) and after (the hydride transfer, 5B in Scheme 2) the formation of an intermediate, increasing the confidence in the existence of that putative intermediate.

ASSOCIATED CONTENT

Supporting Information

The Supporting Information is available free of charge on the ACS Publications website at DOI: 10.1021/acscatal.5b01332.

Tables presenting the observed and intrinsic KIEs for both proton abstraction and hydride transfer in R166 K (PDF)

AUTHOR INFORMATION

Corresponding Author

*Phone: +1 319 335 0234. E-mail: amnon-kohen@uiowa.edu.

Notes

The authors declare no competing financial interest.

ACKNOWLEDGMENTS

This work was supported by NIH (R01GM65368) and NSF (CHE-1149023) to A.K. and the Iowa Center of Biocatalysis and Bioprocessing associated with NIH T32 GM008365 to Z.I.

REFERENCES

(1) Carosati, E.; Tochowicz, A.; Marverti, G.; Guaitoli, G.; Benedetti, P.; Ferrari, S.; Stroud, R. M.; Finer-Moore, J.; Luciani, R.; Farina, D.; Cruciani, G.; Costi, M. P. *J. Med. Chem.* **2012**, *55*, 10272−10276.
(2) Sergeeva, O. A.; Khambatta, H. G.; Cathers, B. E.; Sergeeva, M. V. *Biochem. Biophys. Res. Commun.* **2003**, *307*, 297−300.
(3) Costi, M. P.; Tondi, D.; Rinaldi, M.; Barlocco, D.; Pecorari, P.; Soragni, F.; Venturelli, A.; Stroud, R. M. *Biochim. Biophys. Acta, Mol. Basis Dis.* **2002**, *1587*, 206−214.
(4) Popat, S.; Matakidou, A.; Houlston, R. S. *J. Clin. Oncol.* **2004**, *22*, 529−536.
(5) Salonga, D.; Danenberg, K. D.; Johnson, M.; Metzger, R.; Groshen, S.; Tsao-Wei, D. D.; Lenz, H.-J.; Leichman, C. G.; Leichman, L.; Diasio, R. B.; Danenberg, P. V. *Clin. Cancer Res.* **2000**, *6*, 1322−1327.
(6) Copur, S.; Aiba, K.; Drake, J. C.; Allegra, C. J.; Chu, E. *Biochem. Pharmacol.* **1995**, *49*, 1419−1426.
(7) Wilson, P. M.; Danenberg, P. V.; Johnston, P. G.; Lenz, H.-J.; Ladner, R. D. *Nat. Rev. Clin. Oncol.* **2014**, *11*, 282−298.
(8) Calascibetta, A.; Contino, F.; Feo, S.; Gulotta, G.; Cajozzo, M.; Antona, A.; Sanguedolce, G.; Sanguedolce, R. *J. Nucleic Acids* **2010**, *2010*, 306754.
(9) Phan, J.; Steadman, D. J.; Koli, S.; Ding, W. C.; Minor, W.; Dunlap, R. B.; Berger, S. H.; Lebioda, L. *J. Biol. Chem.* **2001**, *276*, 14170−14177.
(10) Johnston, P. G.; Lenz, H. J.; Leichman, C. G.; Danenberg, K. D.; Allegra, C. J.; Danenberg, P. V.; Leichman, L. *Cancer Res.* **1995**, *55*, 1407−1412.
(11) Carreras, C. W.; Santi, D. V. *Annu. Rev. Biochem.* **1995**, *64*, 721−762.
(12) Newby, Z.; Lee, T. T.; Morse, R. J.; Liu, Y.; Liu, L.; Venkatraman, P.; Santi, D. V.; Finer-Moore, J. S.; Stroud, R. M. *Biochemistry* **2006**, *45*, 7415−7428.
(13) Finer-Moore, J. S.; Santi, D. V.; Stroud, R. M. *Biochemistry* **2003**, *42*, 248−256.
(14) Spencer, H. T.; Villafranca, J. E.; Appleman, J. R. *Biochemistry* **1997**, *36*, 4212−4222.
(15) Agrawal, N.; Hong, B.; Mihai, C.; Kohen, A. *Biochemistry* **2004**, *43*, 1998−2006.
(16) Wang, Z.; Kohen, A. *J. Am. Chem. Soc.* **2010**, *132*, 9820−9825.
(17) Wang, Z.; Ferrer, S.; Moliner, V.; Kohen, A. *Biochemistry* **2013**, *52*, 2348−2358.
(18) Kanaan, N.; Ferrer, S.; Marti, S.; Garcia-Viloca, M.; Kohen, A.; Moliner, V. *J. Am. Chem. Soc.* **2011**, *133*, 6692−6702.
(19) Kanaan, N.; Roca, M.; Tunon, I.; Marti, S.; Moliner, V. *J. Phys. Chem. B* **2010**, *114*, 13593−13600.
(20) Kanaan, N.; Marti, S.; Moliner, V.; Kohen, A. *J. Phys. Chem. A* **2009**, *113*, 2176−2182.
(21) Kanaan, N.; Marti, S.; Moliner, V.; Kohen, A. *Biochemistry* **2007**, *46*, 3704−3713.
(22) Huang, W.; Santi, D. V. *Biochemistry* **1997**, *36*, 1869−1873.
(23) Bruice, T. W.; Santi, D. V. In *Enzyme mechanism from isotope effects*; CRC Press: Boca Raton, 1991; pp 457−479.
(24) Kohen, A. *Acc. Chem. Res.* **2015**, *48*, 466−473.
(25) Klinman, J. P.; Kohen, A. *Annu. Rev. Biochem.* **2013**, *82*, 5543−5567.
(26) Hanoian, P.; Liu, C. T.; Hammes-Schiffer, S.; Benkovic, S. *Acc. Chem. Res.* **2015**, *48*, 482−489.
(27) Layfield, J. P.; Hammes-Schiffer, S. *Chem. Rev.* **2014**, *114*, 3466−3494.

DOI: 10.1021/acscatal.5b01332
ACS Catal. 2015, 5, 6061−6068

(28) Nagel, Z. D.; Klinman, J. P. *Chem. Rev.* **2010**, *110*, PR41−PR67.
(29) Maglia, G.; Allemann, R. K. *J. Am. Chem. Soc.* **2003**, *125*, 13372−13373.
(30) Hay, S.; Scrutton, N. S. *Nat. Chem.* **2012**, *4*, 161−168.
(31) Pudney, C. R.; Hay, S.; Levy, C.; Pang, J.; Sutcliffe, M. J.; Leys, D.; Scrutton, N. S. *J. Am. Chem. Soc.* **2009**, *131*, 17072−17073.
(32) Marcus, R. A. *J. Phys. Chem. B* **2007**, *111*, 6643−6654.
(33) Antoniou, D.; Basner, J.; Nunez, S.; Schwartz, S. D. *Chem. Rev.* **2006**, *106*, 3170−3187.
(34) Roston, D.; Islam, Z.; Kohen, A. *Arch. Biochem. Biophys.* **2014**, *544*, 96−104.
(35) Roston, D.; Islam, Z.; Kohen, A. *Molecules* **2013**, *18*, 5543−5567.
(36) Roston, D.; Cheatum, C. M.; Kohen, A. *Biochemistry* **2012**, *51*, 6860−6870.
(37) Klinman, J. P. *Acc. Chem. Res.* **2015**, *48*, 449−456.
(38) Blakley, R. L. *Nature (London, U. K.)* **1960**, *188*, 231−232.
(39) Changchien, L. M.; Garibian, A.; Frasca, V.; Lobo, A.; Maley, G. F.; Maley, F. *Protein Expression Purif.* **2000**, *19*, 265−270.
(40) Wataya, Y.; Hayatsu, H. *J. Am. Chem. Soc.* **1972**, *94*, 8927−8928.
(41) Cook, P. F.; Cleland, W. W. In *Enzyme kinetics and mechanism*; Garland Science: London, New York, 2007; p 253.
(42) Islam, Z.; Strutzenberg, T. S.; Gurevic, I.; Kohen, A. *J. Am. Chem. Soc.* **2014**, *136*, 9850−9853.
(43) Hong, B.; Maley, F.; Kohen, A. *Biochemistry* **2007**, *46*, 14188−14197.
(44) Ghosh, A. K.; Islam, Z.; Krueger, J. D.; Abeysinghe, T.; Kohen, A. *Phys. Chem. Chem. Phys.* **2015**. http://dx.doi.org/10.1039/C5CP01246E.
(45) Abeysinghe, T.; Kohen, A. *Int. J. Mol. Sci.* **2015**, *16*, 7304−7319.
(46) Northrop, D. B. In *Enzyme mechanism from isotope effects*; CRC Press: Boca Raton, FL, 1991; p 181−202.
(47) Parkin, D. W. In *Enzyme mechanism from isotope effects*; Cook, P. F., Ed.; CRC Press: Boca Raton, 1991; pp 269−290.
(48) Hong, B.; Haddad, M.; Maley, F.; Jensen, J. H.; Kohen, A. *J. Am. Chem. Soc.* **2006**, *128*, 5636−5637.
(49) Wang, Z.; Abeysinghe, T.; Finer-Moore, J. S.; Stroud, R. M.; Kohen, A. *J. Am. Chem. Soc.* **2012**, *134*, 17722−17730.
(50) Swiderek, K.; Kohen, A.; Moliner, V. *Phys. Chem. Chem. Phys.* **2015**. http://dx.doi.org/10.1039/C5CP01239B.
(51) Hyatt, D. C.; Maley, F.; Montfort, W. R. *Biochemistry* **1997**, *36*, 4585−4594.
(52) Kaiyawet, N.; Lonsdale, R.; Rungrotmongkol, T.; Mulholland, A. J.; Hannongbua, S. *J. Chem. Theory Comput.* **2015**, *11*, 713−722.

DOI: 10.1021/acscatal.5b01332
ACS Catal. 2015, 5, 6061−6068